

# A Precise Determination of Electroweak Parameters in Neutrino-Nucleon Scattering

G. P. Zeller<sup>5</sup>, T. Adams<sup>4</sup>, A. Alton<sup>4</sup>, S. Avvakumov<sup>8</sup>, L. de Barbaro<sup>5</sup>, P. de Barbaro<sup>8</sup>,  
R. H. Bernstein<sup>3</sup>, A. Bodek<sup>8</sup>, T. Bolton<sup>4</sup>, J. Brau<sup>6</sup>, D. Buchholz<sup>5</sup>, H. Budd<sup>8</sup>, L. Bugel<sup>3</sup>,  
J. Conrad<sup>2</sup>, R. B. Drucker<sup>6</sup>, B. T. Fleming<sup>2</sup>, R. Frey<sup>6</sup>, J.A. Formaggio<sup>2</sup>, J. Goldman<sup>4</sup>,  
M. Goncharov<sup>4</sup>, D. A. Harris<sup>8</sup>, R. A. Johnson<sup>1</sup>, J. H. Kim<sup>2</sup>, S. Koutsoliotas<sup>2</sup>,  
M. J. Lamm<sup>3</sup>, W. Marsh<sup>3</sup>, D. Mason<sup>6</sup>, J. McDonald<sup>7</sup>, K. S. McFarland<sup>8,3</sup>, C. McNulty<sup>2</sup>,  
D. Naples<sup>7</sup>, P. Nienaber<sup>3</sup>, A. Romosan<sup>2</sup>, W. K. Sakumoto<sup>8</sup>, H. Schellman<sup>5</sup>,  
M. H. Shaevitz<sup>2</sup>, P. Spentzouris<sup>2</sup>, E. G. Stern<sup>2</sup>, N. Suwonjandee<sup>1</sup>, M. Tzanov<sup>7</sup>, M. Vakili<sup>1</sup>,  
A. Vaitaitis<sup>2</sup>, U. K. Yang<sup>8</sup>, J. Yu<sup>3</sup>, and E. D. Zimmerman<sup>2</sup>

<sup>1</sup>*University of Cincinnati, Cincinnati, OH 45221*

<sup>2</sup>*Columbia University, New York, NY 10027*

<sup>3</sup>*Fermi National Accelerator Laboratory, Batavia, IL 60510*

<sup>4</sup>*Kansas State University, Manhattan, KS 66506*

<sup>5</sup>*Northwestern University, Evanston, IL 60208*

<sup>6</sup>*University of Oregon, Eugene, OR 97403*

<sup>7</sup>*University of Pittsburgh, Pittsburgh, PA 15260*

<sup>8</sup>*University of Rochester, Rochester, NY 14627*

(July 7, 2001)

## Abstract

The NuTeV collaboration determines the electroweak parameter  $\sin^2 \theta_W$  by measuring the ratio of neutral current to charged current  $\nu$  and  $\bar{\nu}$  cross-sections. We find  $\sin^2 \theta_W^{(\text{on-shell})} = 0.2274 \pm 0.0014(\text{stat}) \pm 0.0009(\text{syst})$ , a value 2.8 standard deviations above the Standard Model prediction. If we

relax the Standard Model assumption that  $\rho_{NC}^0 = 1$ , we find  $\rho_0 = 1.0009 \pm 0.0041$ . A model independent analysis of the same data in terms of neutral-current quark couplings is also presented.

Neutrino-nucleon scattering is one of the most precise probes of the weak neutral current. The Lagrangian for weak neutral current  $\nu$ - $q$  scattering can be written at tree level as

$$\mathcal{L} = -\frac{G_F \rho_0}{\sqrt{2}} (\bar{\nu} \gamma^\mu (1 - \gamma^5) \nu) \times (\epsilon_L^q \bar{q} \gamma_\mu (1 - \gamma^5) q + \epsilon_R^q \bar{q} \gamma_\mu (1 + \gamma^5) q), \quad (1)$$

where deviations from  $\rho_0$  of 1 describe non-Standard Model sources of SU(2) breaking, and  $\epsilon_{L,R}^q$  are the chiral quark couplings. For the weak charged current,  $\epsilon_L^q = I_{\text{weak}}^{(3)}$  and  $\epsilon_R^q = 0$ , but for the neutral current  $\epsilon_L^q$  and  $\epsilon_R^q$  each have an additional term,  $-Q \sin^2 \theta_W$ , where  $Q$  is the quark electric charge in units of  $e$ . By measuring ratios of the charged and neutral current processes on a hadronic target, one can thus extract  $\sin^2 \theta_W$  and  $\rho_0$ .

In the context of the Standard Model, this measurement of  $\sin^2 \theta_W$  is comparable in precision to direct measurements of  $M_W$ . Outside the Standard Model, neutrino-nucleon scattering provides one of the most precise constraints on the weak couplings of light quarks, and tests the validity of the electroweak theory over many orders of magnitude in momentum transfer squared,  $q^2$ , when compared to on-shell probes of weak bosons. This process is also sensitive to non-Standard Model interactions, including leptoquark and  $Z'$  exchange [1].

The ratio of neutral current to charged current cross-sections for either  $\nu$  or  $\bar{\nu}$  scattering from isoscalar targets of  $u$  and  $d$  quarks can be written as [2]

$$R^{\nu(\bar{\nu})} \equiv \frac{\sigma(\bar{\nu} N \rightarrow \bar{\nu} X)}{\sigma(\nu N \rightarrow \ell^{-(+)} X)} = (g_L^2 + r^{(-1)} g_R^2), \quad (2)$$

where

$$r \equiv \frac{\sigma(\bar{\nu} N \rightarrow \ell^+ X)}{\sigma(\nu N \rightarrow \ell^- X)} \sim \frac{1}{2}, \quad (3)$$

and  $g_{L,R}^2 = (\epsilon_{L,R}^u)^2 + (\epsilon_{L,R}^d)^2$ . In a real target, there are corrections to Eqn. 2 resulting from the presence of heavy quarks in the sea, the production of heavy quarks in the target, non leading-order quark-parton model terms in the cross-section, electromagnetic radiative corrections, and any isovector component of the light quarks in the target. In particular, in the case where a final-state charm quark is produced from a  $d$  or  $s$  quark in the nucleon, the

uncertainties resulting from the mass suppression of the heavy charm quark are large. The uncertainty in this suppression ultimately limited the precision of previous neutrino-nucleon scattering experiments which measured electroweak parameters [3–5].

To reduce the effect of uncertainties resulting from charm production, one can instead consider a quantity suggested by Paschos and Wolfenstein [6],

$$\begin{aligned} R^- &\equiv \frac{\sigma(\nu_\mu N \rightarrow \nu_\mu X) - \sigma(\bar{\nu}_\mu N \rightarrow \bar{\nu}_\mu X)}{\sigma(\nu_\mu N \rightarrow \mu^- X) - \sigma(\bar{\nu}_\mu N \rightarrow \mu^+ X)} \\ &= \frac{R^\nu - r R^{\bar{\nu}}}{1 - r} = (g_L^2 - g_R^2). \end{aligned} \quad (4)$$

$R^-$  is a more difficult quantity to measure than  $R^\nu$ , primarily because neutral current  $\nu$  and  $\bar{\nu}$  scattering have identical observed final states and can only be separated by *a priori* knowledge of the initial state neutrino.

## METHOD

High-purity  $\nu$  and  $\bar{\nu}$  beams were provided by the Sign Selected Quadrupole Train (SSQT) beamline at the Fermilab Tevatron during the 1996-1997 fixed target run. Neutrinos are produced from the decay of pions and kaons resulting from interactions of 800 GeV protons in a BeO target. Dipole magnets immediately downstream of the proton target bend pions and kaons of specified charge in the direction of the NuTeV detector, while oppositely charged and neutral mesons are stopped in beam dumps. The resulting beam is almost purely  $\nu$  or  $\bar{\nu}$ , depending on the selected sign of the parent mesons.  $\bar{\nu}$  interactions comprise less than 0.1% of the neutrino beam events, and  $\nu$  interactions are less than 0.5% of the observed rate in the anti-neutrino beam. In addition, the beam is almost purely muon neutrino, with electron neutrinos (mostly from  $K_{e3}^\pm$  decays) creating 1.8% of the observed interactions in each of the neutrino and anti-neutrino beams.

Neutrino interactions are observed in the NuTeV detector [8], located approximately 1.5 km downstream of the proton target. The detector consists of an 18m long, 690 ton steel-scintillator target followed by an instrumented iron-toroid spectrometer. The target

calorimeter is composed of 168 3 m x 3 m x 5.1 cm steel plates interspersed with liquid scintillation counters (spaced every two plates) and drift chambers (spaced every four plates). The scintillation counters provide triggering information as well as a determination of the longitudinal event vertex, event length, and visible energy deposition. The mean position of hits in the drift chambers establish the transverse event vertex. The toroidal spectrometer, which determines muon charge and momentum, is used for muon neutrino flux measurement in charged current events. In addition, the detector was continuously calibrated through exposure to a wide energy range of test beam hadrons, electrons, and muons [8].

For inclusion in this analysis, events are required to deposit at least 15 GeV of visible energy ( $E_{\text{cal}}$ ) in the calorimeter; this ensures full efficiency of the event trigger, proper vertex determination, and reduction of cosmic ray background events. Fiducial cuts restrict the location of the neutrino interaction to the central region of the calorimeter, excluding events that begin in the first 4 counters or in the last 20% of the detector. The chosen volume selects interactions that were contained in the calorimeter, and it minimizes the fraction of events from electron neutrinos or non-neutrino sources.

After all cuts, the resulting data sample consists of  $1.87 \times 10^6$   $\nu$  and  $0.42 \times 10^6$   $\bar{\nu}$  events with a mean visible energy,  $E_{\text{cal}}$ , of 68 GeV and 51 GeV, respectively.

In order to measure  $\sin^2 \theta_W$ , the observed neutrino events must be separated into charged current (CC) and neutral current (NC) candidates. Both CC and NC neutrino interactions initiate a cascade of hadrons in the target that is registered in both the scintillation counters and drift chambers. Muon neutrino CC events are distinguished by the presence of a final state muon. The muon typically penetrates well beyond the hadronic shower and deposits energy in a large number of consecutive scintillation counters. NC events usually have no final state muon and deposit energy over a range of counters typical of a hadronic shower.

These differing event topologies enable the statistical separation of CC and NC neutrino interactions based solely on event length. For each event, the length is defined as the number of scintillation counters between the interaction vertex and the last counter consistent with at least single muon energy deposition. Events with a “long” length are identified as CC

candidates; other “short” events are most likely NC induced. The separation between short and long events is made at 16 counters if  $E_{\text{cal}} < 55$  GeV, at 17 counters if  $55 \leq E_{\text{cal}} < 100$  GeV, and otherwise at 18 counters. The ratios of short to long events measured in the  $\nu$  and  $\bar{\nu}$  beams are:

$$R_{\text{exp}}^{\nu} = 0.3926 \pm 0.0007 \text{ and } R_{\text{exp}}^{\bar{\nu}} = 0.4037 \pm 0.0015. \quad (5)$$

$\sin^2 \theta_W$  can be directly extracted from these measured ratios by comparison with a detailed Monte Carlo (MC) simulation of the experiment. The Monte Carlo must include neutrino fluxes, the neutrino cross sections, and a detailed description of the detector response. The remaining sections will describe these three components.

A detailed beam simulation is used to predict the  $\nu$  and  $\bar{\nu}$  fluxes. In particular, a precise determination of the electron neutrino contamination in the beam is essential. The ratios  $R_{\text{exp}}^{\nu}$  and  $R_{\text{exp}}^{\bar{\nu}}$  are increased by the presence of electron neutrinos in the data sample because their charged current interactions, which usually lack an energetic muon in the final state, are almost always identified as neutral current interactions in the detector.

The bulk, 93% in the  $\nu$  beam and 70% in the  $\bar{\nu}$  beam, of the observed electron neutrinos result from  $K_{e3}^{\pm}$  decays. The beam simulation can be tuned to describe  $\nu_e$  and  $\bar{\nu}_e$  production from charged kaon decay with high accuracy given that the  $K^{\pm}$  decay contribution is constrained by measurements of the observed  $\nu_{\mu}$  and  $\bar{\nu}_{\mu}$  fluxes. Because of the precise alignment of the beamline elements and the low acceptance for neutral particle propagation in the SSQT, the largest uncertainty in the calculated electron neutrino flux is the 1.1% uncertainty in the  $K_{e3}^{\pm}$  branching ratio [9]. Other sources of electron neutrinos include neutral kaons, charmed hadrons and muon decay, all of which have larger fractional uncertainties (10-20%). Finally, small detector calibration uncertainties in the calorimeter hadron and muon toroid energy scales affect the muon and electron neutrino fluxes. Additional constraints from the data itself, including direct measurements of  $\nu_e$  and  $\bar{\nu}_e$  charged current events and measurements of  $\nu_{\mu}$  events in the  $\bar{\nu}_{\mu}$  beam (which also result from charm and neutral kaon decay) [7] reduce the electron neutrino uncertainties.

Neutrino-nucleon deep inelastic scattering processes are simulated using a leading order (LO) cross section model augmented with longitudinal scattering and higher twist terms. The cross section parametrization incorporates LO parton momentum distributions (PDFs) from CCFR charged current data measured using the same target and cross section model as NuTeV [10,11]. These PDFs include an external constraint on  $\sigma^{\bar{\nu}}/\sigma^{\nu}$  [11]. Small modifications adjust the parton densities to produce the inherent up-down quark asymmetry consistent with muon scattering [12] and Drell-Yan [13] data. A LO analysis of  $(\bar{\nu}) N \rightarrow \mu^+ \mu^- X$  events in CCFR and NuTeV [14] provides the shape and magnitude of the strange sea. Mass suppression from charged current charm production is modeled using a LO slow rescaling formalism [15] whose parameters and uncertainties come from the same high-statistics  $\mu^+ \mu^-$  sample. The charm sea is chosen to match EMC data [16] with a slow-rescaling parameter of  $2m_c$ ; it is assigned a 100% uncertainty. A global analysis [17] provides a parameterization of the longitudinal structure function,  $R_L$ , which is varied by its experimental and theoretical uncertainties. Electroweak and QED radiative corrections to the scattering cross section are applied using code supplied by Bardin [18], and uncertainties are estimated by varying parameters of these corrections.

The Monte Carlo must also accurately simulate the response of the detector to the products of neutrino interactions in the target. The critical detector parameters that must be modeled are the calorimeter response to muons, measurement of the neutrino interaction position, and the range of hadronic showers in the calorimeter. Precise determination of these effects are made possible through extensive use of both neutrino and testbeam data. Measured detector parameters are then varied within their uncertainties to study systematic errors associated with their simulation.

An important test of the simulation is its ability to predict the length distribution of events in the detector. Figure 1 shows event length distributions of the final data sample compared to the Monte Carlo prediction with our measured  $\sin^2 \theta_W$ . Events reaching the toroid, which comprise about 80% of the CC sample, have been left out for clarity, but are included in the normalization of the data.

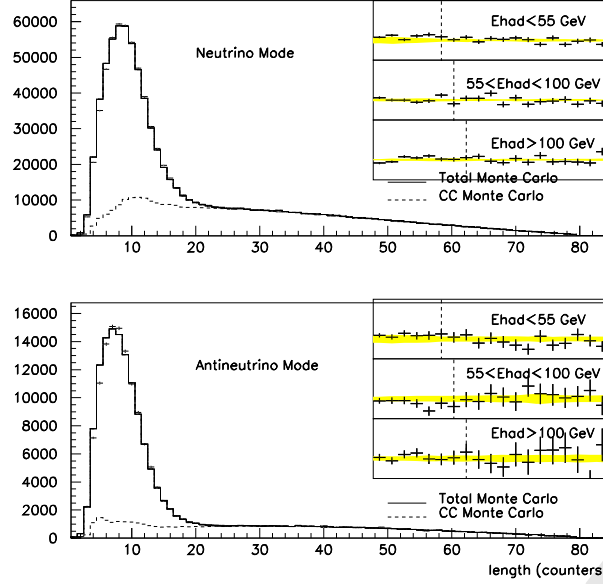


FIG. 1. Comparison of  $\nu$  and  $\bar{\nu}$  event length distributions in data and Monte Carlo (MC). The MC prediction for CC events is shown separately. Insets show data/MC ratio comparisons in the region of the length cut with bands to indicate the  $1\sigma$  systematic uncertainty in this ratio.

## RESULTS

Having precisely determined  $R_{\text{exp}}^\nu$ ,  $R_{\text{exp}}^{\bar{\nu}}$ , and their predicted values as a function of electroweak parameters  $\sin^2 \theta_W$  and  $\rho_0$ , we proceed to extract the values of  $\sin^2 \theta_W$  and  $\rho_0$ . This is done by means of a fit that also includes the value of the slow-rescaling mass for charm production,  $m_c$ , with its *a priori* constraint from  $\mu^+\mu^-$  data [14].  $R^{\bar{\nu}}$  is much less sensitive to  $\sin^2 \theta_W$  than  $R^\nu$ , but both are sensitive to  $m_c$  and  $\rho_0$ .

When fitting with the Standard Model assumption  $\rho_0 = 1$ ,  $\sin^2 \theta_W$  is effectively determined through the linear combination  $R^\nu - 0.262R^{\bar{\nu}}$ . As with  $R^-$ , this combination minimizes uncertainties related to charm production suppression, and reduces uncertainties related to sea quark scattering and many experimental systematics common to both  $\nu$  and  $\bar{\nu}$  samples. When fitting with  $\rho_0$  as a second free parameter, systematic uncertainties will be larger, because this cancellation of uncertainties is not realized. Statistical and systematic uncertainties from the  $\sin^2 \theta_W$  and  $\sin^2 \theta_W - \rho_0$  fits are shown in Table I.

The single parameter fit for  $\sin^2 \theta_W$  measures:



SOURCE OF UNCERTAINTY	$\delta \sin^2 \theta_W$	$\delta \sin^2 \theta_W$	$\delta \rho_0$
Data Statistics	0.00141	0.00281	0.00354
Monte Carlo Statistics	0.00001	0.00001	0.00001
<b>TOTAL STATISTICS</b>	0.00141	0.00281	0.00354
$\nu_e, \bar{\nu}_e$ Flux	0.00036	0.00124	0.00163
Energy Measurement	0.00031	0.00039	0.00038
Shower Length Model	0.00030	0.00004	0.00037
Counter Efficiency, Noise, Size	0.00018	0.00019	0.00005
Longitudinal Vertex	0.00047	0.00030	0.00024
Transverse Vertex	0.00011	0.00009	0.00005
<b>TOTAL EXPERIMENTAL</b>	0.00077	0.00135	0.00173
Charm Production, $s(x)$	0.00014	0.00033	0.00063
Charm Sea	0.00019	0.00017	0.00002
$\sigma^{\bar{\nu}}/\sigma^{\nu}$	0.00024	0.00048	0.00036
Radiative Corrections	0.00011	0.00019	0.00011
Non-Isoscalar Target	0.00005	0.00002	0.00004
Higher Twist	0.00010	0.00001	0.00014
$R_L$	0.00029	0.00061	0.00130
<b>TOTAL MODEL</b>	0.00047	0.00088	0.00150
<b>TOTAL UNCERTAINTY</b>	0.00164	0.00316	0.00413

TABLE I. Uncertainties for both the single parameter  $\sin^2 \theta_W$  fit and the two parameter, simultaneous  $\sin^2 \theta_W - \rho_0$  fit.

$$\begin{aligned}
\sin^2 \theta_W^{(\text{on-shell})} &= 0.2274 \pm 0.0014(\text{stat.}) \pm 0.0009(\text{syst.}) \\
&\quad - 0.00088 \times \left( \frac{M_{\text{top}}^2 - (175 \text{ GeV})^2}{(100 \text{ GeV})^2} \right) \\
&\quad + 0.00032 \times \ln\left( \frac{M_{\text{Higgs}}}{150 \text{ GeV}} \right)
\end{aligned} \tag{6}$$

Leading terms in the one-loop electroweak radiative corrections [18] to the W and Z self energies produce the small residual dependence of our result on  $M_{\text{top}}$  and  $M_{\text{Higgs}}$ . The Standard Model prediction from Electroweak fits is  $0.2227 \pm 0.00037$  [19,20], approximately  $2.8\sigma$  from our result. In the on-shell scheme,  $\sin^2 \theta_W \equiv 1 - M_W^2/M_Z^2$ , where  $M_W$  and  $M_Z$  are the physical gauge boson masses, our result implies  $M_W = 80.151 \pm 0.082$  GeV, compared with the world-average direct measurement of  $M_W = 80.446 \pm 0.040$  GeV [19].

For the simultaneous  $\sin^2 \theta_W - \rho_0$  fit,

$$\rho_0 = 1.0009 \pm 0.0041, \quad \sin^2 \theta_W = 0.2281 \pm 0.0032, \tag{7}$$

with correlation coefficient of 0.86 between the two parameters. One can also perform the two-parameter fit in terms of the isoscalar combinations<sup>1</sup> of effective neutral-current quark couplings  $g_L^{\text{eff}^2}$  and  $g_R^{\text{eff}^2}$  at  $\langle q^2 \rangle \approx -20$  GeV<sup>2</sup>. That result is:

$$(g_L^{\text{eff}})^2 = 0.3010 \pm 0.0014, \quad (g_R^{\text{eff}})^2 = 0.0317 \pm 0.0012, \tag{8}$$

with a correlation coefficient of approximately zero. Standard Model expectations for these couplings are  $g_L^{\text{eff}^2} = 0.3038$  and  $g_R^{\text{eff}^2} = 0.0301$  [21].

In conclusion, NuTeV has made precision determinations of the electroweak parameters  $\sin^2 \theta_W$  and  $\rho_0$  through separate measurements of  $R^\nu$  and  $R^{\bar{\nu}}$ . We find a significant disagreement with the Standard Model expectation for  $\sin^2 \theta_W^{(\text{on-shell})}$ . In a model-independent analysis, this result suggests smaller left-handed and larger right-handed neutral current couplings of the light quarks than expected.

---

<sup>1</sup>This result is only sensitive to isovector combinations at about 3% of the sensitivity of isoscalar couplings, due to the asymmetry between the strange and charm seas and to the slight excess of neutrons in our target.

## ACKNOWLEDGEMENTS

We wish to thank the staff of the Fermilab Beams, Computing and Particle Physics divisions for design, construction, and operational assistance during the NuTeV experiment. This work was supported by the U.S. Department of Energy, the National Science Foundation and the Alfred P. Sloan foundation.

## REFERENCES

- [1] P. Langacker *et al.*, Rev. Mod. Phys. **64**, 87 (1991).
- [2] C. H. Llewellyn Smith, Nucl. Phys. **B228**, 205 (1983).
- [3] K. S. McFarland *et al.*, Eur. Phys. Jour. **C1**, 509 (1998).
- [4] A. Blondel *et al.*, Zeit. Phys. **C45**, 361 (1990).
- [5] J. Allaby *et al.*, Zeit. Phys. **C36**, 611 (1985.).
- [6] E. A. Paschos and L. Wolfenstein Phys. Rev. **D7**, 91 (1973).
- [7] A. Alton *et al.*, eprint hep-ex/0008068, submitted to PRD.
- [8] D. A. Harris and J. Yu *et al.*, Nucl. Instr. Meth. **A447**, 373 (2000).
- [9] D.E. Groom *et al.*, Eur. Phys. Jour. **C15**, 1 (2000.). Measurements of  $K^\pm$  and  $K_L$  partial widths are combined, allowing for isospin-violation uncertainties.
- [10] A. J. Buras and K. J. F. Gaemers, Nucl. Phys. **B132**, 249 (1978).
- [11] U. K. Yang *et al.*, Phys. Rev. Lett. **86**, 2742 (2001).
- [12] M. Arneodo *et al.*, Nucl. Phys. **B487**, 3 (1997).
- [13] E. A. Hawker *et al.*, Phys. Rev. Lett. **80**, 3715 (1998).
- [14] M. Goncharov *et al.*, eprint hep-ex/0102049, submitted to PRD, February 2001.
- [15] R. M. Barnett, Phys. Rev. Lett. **36**, 1163 (1976.).
- [16] J. J. Aubert *et al.*, Nucl. Phys. **B213**, 31 (1983).
- [17] L. W. Whitlow, SLAC-REPORT-357, 109 (1990).
- [18] D. Yu. Bardin and V. A. Dokuchaeva, JINR-E2-86-260, (1986).
- [19] “A Combination of Preliminary Electroweak Measurements and Constraints on the Standard Model”, LEPEWWG/2001-01 (unpublished)

[20] M. Gruenewald, private communication, for the fit of Ref. [19] without the NuTeV preliminary result included.

[21] D.E. Groom *et al.*, Eur. Phys. Jour. **C15**, 1 (2000.).

Internal NuTeV DRAFT